Journal of Solid State Chemistry 235 (2016) 43–49

Contents lists available at ScienceDirect

Journal of Solid State Chemistry

journal homepage: www.elsevier.com/locate/jssc

Electrochemical properties of copper-based compounds with polyanion frameworks

Yoshifumi Mizuno, Shoma Hata, Kota Suzuki, Masaaki Hirayama, Ryoji Kanno*

Department of Electronic Chemistry, Tokyo Institute of Technology, G1-1, 4259, Nagatsuta, Midori-ku, Yokohama, Kanagawa 226-8502, Japan

ARTICLE INFO

Article history:
Received 3 September 2015
Received in revised form
1 December 2015
Accepted 3 December 2015
Available online 7 December 2015

Keywords:
Lithium battery
Electrode material
Polyanion compound

ABSTRACT

The copper-based polyanion compounds $Li_6CuB_4O_{10}$ and $Li_2CuP_2O_7$ were synthesized using a conventional solid-state reaction, and their electrochemical properties were determined. $Li_6CuB_4O_{10}$ showed reversible capacity of 340 mA g^{-1} at the first discharge–charge process, while $Li_2CuP_2O_7$ showed large irreversible capacity and thus low charge capacity. *Ex situ* X-ray diffraction (XRD) and X-ray absorption near edge structure (XANES) measurements revealed that the electrochemical Li^+ intercalation/deintercalation reaction in $Li_6CuB_4O_{10}$ occurred *via* reversible Cu^{2+}/Cu^+ reduction/oxidation reaction. These differences in their discharge/charge mechanisms are discussed based on the strength of the Cu–O covalency *via* their inductive effects.

1. Introduction

Copper-based materials have attracted attention as low-cost and safe electrodes for lithium batteries [1–10]. Among them, Li_2CuO_2 shows large charge capacity of 490 mAh g^{-1} at the first cycle, which is very close to the theoretical capacity of the bi-electron reaction. Although high charge capacity was observed, an irreversible structural change, which occurred during the first charge process, resulted in a large irreversible capacity at the first charge–discharge cycle, which provides poor cycle stability [11]. Therefore, more stable Cu-based electrode materials with robust frameworks are necessary for enhancing cycle stability.

For the enhancement of the cycle stability of Cu-based electrode materials, we have been focused on polyanion compounds. Goodenough et al. reported that Fe-based polyanion compounds could be stabilized by introducing polyanions, $(XO_4)^{n-}$ (X=S, P, Si, As, etc.), into their lattice [12]. Furthermore, introduction of these polyanions increases the Fe^{2+}/Fe^{3+} redox potential because the X–O bonds increased the electronegativity of the anionic group, enhancing the ionic character of the M–O bonds [13,14]. The inductive effect provides excellent cycle stability and high charge–discharge potentials in Fe-based polyanion cathode compounds, such as $LiFePO_4$ [15], $Li_2FeP_2O_7$ [16], Li_2FeSiO_4 [17], and $LiFeBO_3$ [18]. This effect suggests that energy densities as well as cycle stability of Cu-based electrode materials may be enhanced. Recently, Ceder et al. reported the redox potentials for Cu^{2+}/Cu^{3+} and Cu^+/Cu^{2+} couples in the phosphate framework based on *ab initio* calculation [19]. Although the much higher redox potential of the Cu^{2+}/Cu^{3+} couple is greater than 4.5 V, that for the Cu^+/Cu^{2+} couple is approximately 3.2 V, which is suitable for lithium batteries with organic electrolytes. In addition, the low-valent redox couple of Cu^+/Cu^{2+} is likely to have high charge–discharge capacity because the low-valent cation redox couple requires small amounts of polyanions to form the framework. The present report focuses on two polyanion compounds containing Cu^{2+}, $Li_6CuB_4O_{10}$ [20,21], and $Li_2CuP_2O_7$ [22]. Fig. 1 shows crystal structures for $Li_6CuB_4O_{10}$ and $Li_2CuP_2O_7$. Both compounds contain Cu^{2+} in CuO_4 square planes, which are formed with corner-shared BO_3 trihedrons and PO_4 tetrahedras, respectively. The crystal structures indicated that lithium can diffuse along the *a* axis for $Li_6CuB_4O_{10}$ and along the *b* and *c* axes for $Li_2CuP_2O_7$. Therefore, both materials can be expected to undergo electrochemical Li^+ intercalation/deintercalation reactions. Thus, the electrochemical properties for $Li_6CuB_4O_{10}$ and $Li_2CuP_2O_7$ were investigated.

2. Material and methods

$Li_6CuB_4O_{10}$ and $Li_2CuP_2O_7$ were prepared by solid-state reaction as reported previously [20,22]. For $Li_6CuB_4O_{10}$, Li_2CO_3 (99.0%, Wako Chemicals), CuO (98.0%, Kanto Reagents), and H_3BO_3 (99.5%, Kanto Reagents) were mixed in a stoichiometric ratio. The mixture was pelletized and heat-treated at 590 °C for 2 days with intermediate remixing. For $Li_2CuP_2O_7$, stoichiometric amounts of Li_2CO_3 (99.0%, Wako Chemicals), CuO (98.0%, Kanto Reagents), and

* Corresponding author.
E-mail address: kanno@echem.titech.ac.jp (R. Kanno).

http://dx.doi.org/10.1016/j.jssc.2015.12.003
0022-4596/

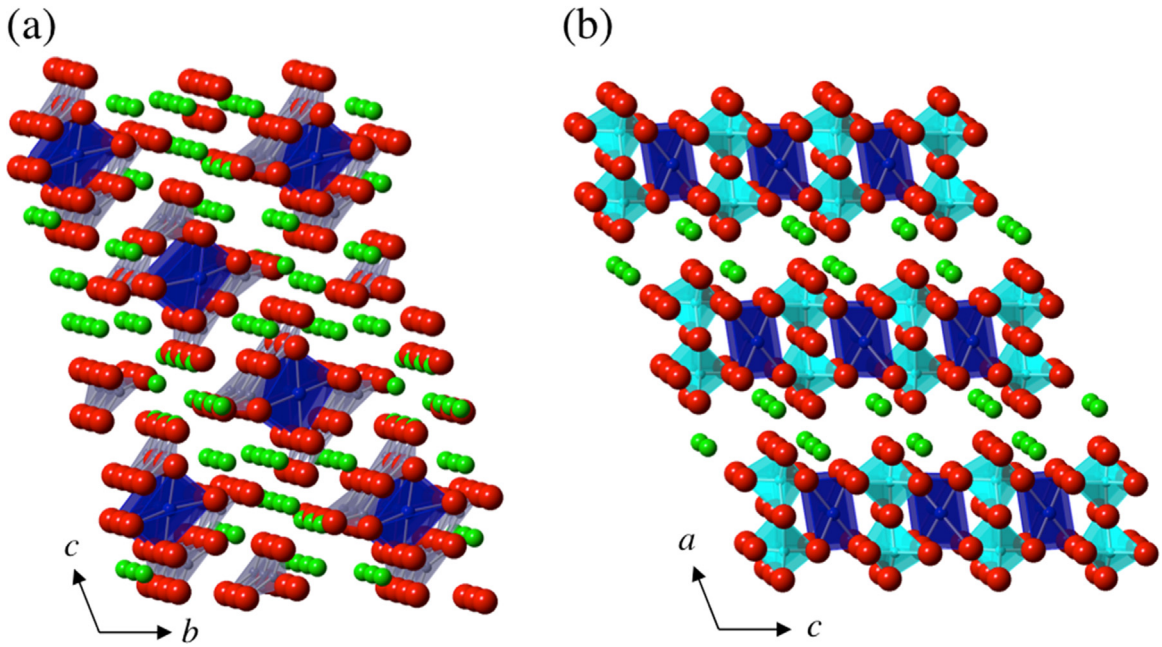

Fig. 1. Crystal structures of (a) $Li_6CuB_4O_{10}$ and (b) $Li_2CuP_2O_7$ (Cu, blue square planes; Li, green spheres; O, red spheres; B, grey trihedrons; P, cyan tetrahedras). (For interpretation of the references to colour in this figure legend, the reader is referred to the web version of this article.)

$(NH_4)_2HPO_4$ (99.0%, Kanto Reagents) were mixed using a planetary ball mill (Fritsch, Premium line P-7) in ethanol for 7 h at 400 rpm. After evaporation of the ethanol, the precursor was pelletized and heat-treated at 590 °C for 12 h.

Powder X-ray diffraction (XRD) measurements were conducted on a Rigaku SmartLab instrument using CuKα radiation in steps of 0.01° over the 2θ range of 10–70°. Synchrotron XRD measurements using a high-flux X-ray source were conducted using BL02B2 and BL19B2 beamlines, SPring-8. Wavelengths of the X-rays were set to $\lambda = 0.6$ (BL02B2) and 0.5 Å (BL19B2). Rietveld analyses for the synchrotron X-ray diffraction patterns were performed using the RIETAN-FP programme [23]. Scanning electron microscopy (SEM) images were obtained on a JEOL JSM-6610LV electron microscope. X-ray absorption spectroscopy (XAS) measurements were performed at the BL14B2 beamline, SPring-8. The spectra were recorded in transmission mode.

For the electrochemical measurements, a 2032 coin-cell battery was used. $Li_6CuB_4O_{10}$ and $Li_2CuP_2O_7$ were mixed with 40 wt% of Ketjen black using a planetary ball-mill (Fritsch, Premium line P-7) with agate balls for 4 h at 240 rpm. The weight ratio of the mixture to the balls was 1:20. The $Li_6CuB_4O_{10}$ underwent additional mixing in a vibrating mill (CMT, TI-100) for 30 min. The final products were mixed with 10 wt% polyvinylidene fluoride (PVdF) in N-methyl-2-pyrrolidone (NMP). The resulting slurries were cast on an Al sheet and dried *in vacuo* at 120 °C for 6 h. Lithium metal was used for the anode, and 1 M $LiPF_6$ in 3:7 (v/v) ethylene carbonate (EC) and diethyl carbonate (DEC) was used as the electrolyte. Charge–discharge measurements were conducted in the potential range of 1.0–4.0 V (*vs.* Li/Li^+). Current density was 30 mA g^{-1}.

3. Results and discussion

3.1. Structural characterization and morphology

$Li_6CuB_4O_{10}$ was synthesized using a solid-state reaction. To determine the crystal structure, Rietveld analysis of the synchrotron XRD pattern was performed. Two polymorphs for this material at room temperature have been reported [20,21]. Rietveld analysis of the synchrotron XRD patterns proceeded using the space group $P-1$, and refinement provided a good agreement factor of $R_{wp} = 6.88$ with a goodness-of-fit value S of 1.86. The refinement patterns and structural parameters are shown in Fig. S1(a) and Table S1(a).

To enhance electronic conductivity, $Li_6CuB_4O_{10}$ was mixed with Ketjen black using a ball mill. Fig. 2 shows the XRD patterns for pristine $Li_6CuB_4O_{10}$, the composite with Ketjen black after ball milling, and the composite with Ketjen black after treatment in the vibrating mill. After ball milling, broad peaks appeared at $2\theta = 13°$, 28°, and 30°, corresponding to 001, $12-1$, and $11-4$ reflections of $Li_6CuB_4O_{10}$, respectively. This peak broadening may indicate a decrease in particle size. The secondary SEM images for pristine $Li_6CuB_4O_{10}$ and the composite obtained with the ball mill are shown in Fig. 3(a) and (b). Before milling, $Li_6CuB_4O_{10}$ had an inhomogeneous particle size of about 5–10 μm. After ball milling, the composite image indicated that the $Li_6CuB_4O_{10}$ particles were well mixed with the Ketjen black. However, the SEM backscattering electron image for the composite indicated that the size of $Li_6CuB_4O_{10}$ particles was similar to that of pristine $Li_6CuB_4O_{10}$, despite the peak broadening observed in the diffraction pattern (Fig. 3(c)). Therefore, the vibrating milling was used for further grinding of the $Li_6CuB_4O_{10}$ particles. The XRD pattern for the composite obtained after treatment in the vibrating mill also is shown in Fig. 2. In the pattern for the composite, broad peaks appeared at $2\theta = 13°$ and 30°, corresponding to the 001 and $11-4$ reflections of $Li_6CuB_4O_{10}$, respectively. These results indicate that the borate-based framework of $Li_6CuB_4O_{10}$ was maintained, even after treatment in the vibrating mill. In addition, the SEM images for the composite showed that the $Li_6CuB_4O_{10}$ particles were mixed well with Ketjen black, and that the $Li_6CuB_4O_{10}$ particles decreased to submicron size (Fig. 3(d) and (e)).

$Li_2CuP_2O_7$ also was synthesized by a solid-state reaction. For $Li_2CuP_2O_7$, only one structural model with the space group of $C2/c$ has been reported [22]. Therefore, Rietveld analysis of the synchrotron XRD pattern was performed. The refinement pattern and structural parameters are shown in Fig. S2 and Table S2, respectively. The profile fitting provided a good agreement factor of $R_{wp} = 6.13$, with a goodness-of-fit value of $S = 1.90$.